ELSEVIER

Journal of Molecular Catalysis A: Chemical 115 (1997) 389–403

JOURNAL OF MOLECULAR CATALYSIS A: CHEMICAL

New directions of catalysis research [1]

Gabor A. Somorjai [*], Michael X. Yang

Department of Chemistry and Materials Sciences Division, Lawrence Berkeley National Laboratory, University of California at Berkeley, Berkeley, CA 94720, USA

Abstract

A variety of surface science technologies have been applied on catalysis studies, in an effort to understand surface structure, composition and chemical bonding in catalytic reactions at a molecular level. Many of the characterizations, however, were performed in vacuum before and after the reactions. A new direction in surface science and catalysis is to study the surface structures and surface intermediates in situ during the high pressure/high temperature reactions. Scanning tunneling microscopy (STM) and infrared–visible sum frequency generation (SFG) are viable for the task. In order to obtain a better comprehension of industrial catalysts, model supported catalysts with ordered structures should be introduced into catalysis research. Metal clusters of uniform size and separation can be produced on oxide surfaces by lithographic microfabrication technologies.

Keywords: Chemical bonding; Lithographic techniques; Scanning tunneling microscopy; Sum frequency generation; Surface science

1. Introduction

1.1. Surface science approach to heterogeneous catalysis

Most chemical energy conversion technologies in the chemical and pharmaceutical industries adapt catalysts to generate products with high rates and desirable selectivity. It was estimated recently that 20% of industrial products involve catalytic steps in their manufacture [1].

In the mid 70's, advances in science instrumentation brought surface science into catalysis research [2]. A high pressure reaction cell was incorporated with an ultra high vacuum (UHV) chamber (Fig. 1). In the high pressure reactor, catalytic reactions can be performed under conditions identical to industrial processes (1–100 atm of reactant gases, 300–1000 K temperature range, variable flow rate or batch reactor conditions). The reaction kinetics and product distribution can be monitored by a gas chromatograph. The samples can be properly cleaned and characterized in UHV by surface science techniques before and after the reactions.

The development of modern surface science provides an opportunity to investigate the process of heterogeneous catalysis at a molecular level. Much progress has been achieved in understanding the mechanisms of a good number of catalytic reactions, notably in the area of ammonia synthesis [3], hydrocarbon reactions [4], hydrodesulfurization [5], CO oxidation [6] and hydrogenation [7], and NO reduction [8]. The understanding of surface chemistry at gas–solid interfaces is beneficial to improvement of

* Corresponding author.

[1] Communication presented at the First Francqui Colloquium, Brussels, 19–20 February 1996.

PII S1381-1169(96)00346-9

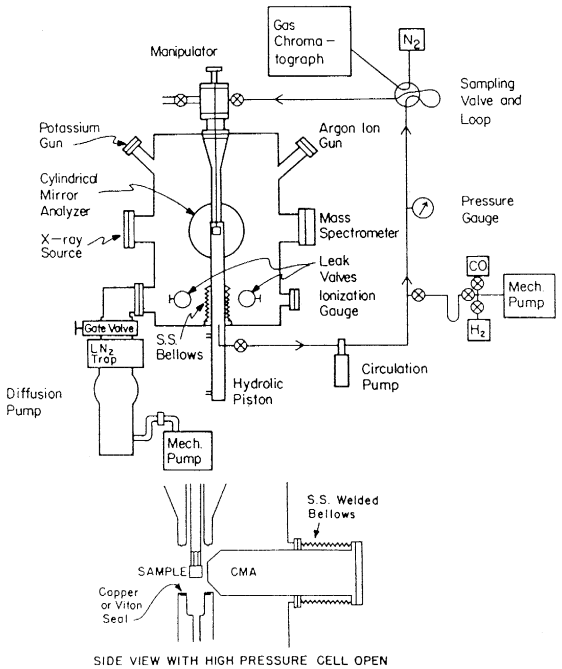

Fig. 1. An apparatus for surface science studies of heterogeneous catalysis: a high pressure environmental cell incorporated with a UHV system.

existing catalysts and development of new generations of catalysts.

1.2. Application of model catalysts in surface science studies

Most industrial catalysts are small metal particles with sizes in the 1–100 nm range deposited on porous oxide supports with a high surface area of $\sim 300\ m^2\ g^{-1}$. They are usually prepared through chemical routes (such as impregnation and coprecipitation) from solution. These conventional fabrication techniques have only limited control of particle size, shape and inter-particle distances. A detailed investigation of catalytic processes is often hindered by the complexity of catalyst surface composition and structure.

In order to comprehend heterogeneous catalysis at a molecular level, model catalysts have been prepared and studied. Single crystal metal surfaces are the first group of novel model catalysts adapted in catalysis research. The advantage of using single crystal surfaces is their homogeneous surface structure and composition.

There are several examples of catalytic reactions where the kinetic parameters and product distributions are insensitive to surface structures of catalysts. For these structure-insensitive processes, reaction rates measured on single crystal surfaces are in good agreement with those obtained on industrial supported catalysts. One example is hydrogenation of cyclohexene, which presents a similar reaction kinetics on a Pt (223) surface [9] and on platinum catalysts on silica support [10] (Fig. 2).

Cleanliness and composition of single crystal surfaces can be well controlled and studied in vacuum. The reactivities of clean surfaces can be treated as an upper limit for those of supported catalysts [11]. Single crystal surfaces can be also fabricated with different concentration of surface contaminants, in order to address origins of catalyst poisoning. In a similar manner, promoters can be deposited on single crystal surfaces to study the modification of catalytic reactivity by additives.

The surface of metal particles in a dispersed catalyst system can be viewed as superposition

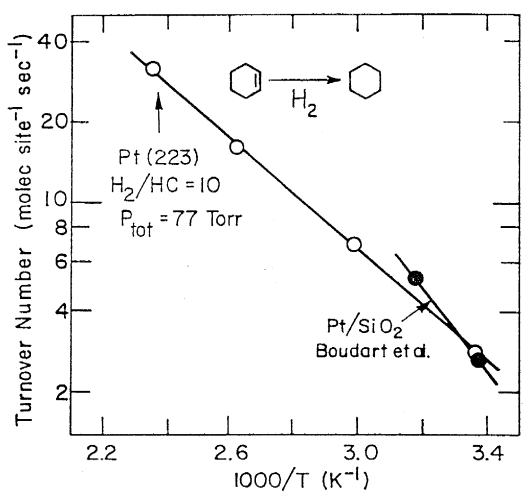

Fig. 2. Arrhenius plot for cyclohexene hydrogenation over Pt(223) and Pt/SiO_2.

of several different single-crystal surfaces. Each surface orientation possesses a different reactivity, and the product distribution reflects the overall chemistry averaged over different surface sites. The surface structure sensitivity of reactions can be addressed in part by studying reactivities of different single crystal faces. The surface irregularities, steps, and kinks of known concentration can be also prepared on high-Miller-index single crystal surfaces.

In addition to single crystals, model metal catalysts can be prepared in thin film form [12–14]. More complex oxide catalysts such as Fe_3O_4 or TiO_2 can be grown by atomic layer epitaxy on metal single-crystal surfaces [15,16]. Recently, model Ziegler–Natta ethylene or propylene polymerization catalysts have been prepared successfully by gas phase deposition of ultra-thin $TiCl_4/MgCl_2$ films in UHV conditions [17]. It is now well accepted that model catalyst behavior can be used as a standard for the evaluation of industrial catalyst systems.

2. Surface science techniques to study the model catalyst surface during reaction

The objective of surface science studies is to investigate elementary steps and detect surface intermediates in catalytic reactions on the molecular level. A wide range of surface science techniques have been developed to probe surface structure, composition and chemical bonding of adsorbates on the surface. A selection of surface analytical techniques are listed in Table 1. Many techniques (including all electron- and ion-scattering spectroscopies) can only be operated in vacuum. As a result, some surface characterizations can only be conducted before and after the high pressure catalytic reactions.

An alternative approach is to study surface reaction mechanisms of organic monolayers prepared in vacuum. The research is often conducted at cryogenic temperatures in order to condense monolayer molecules on the surface.

Table 1
Common surface science techniques for catalysis studies

Electron-mediated spectroscopies
X-ray photoelectron spectroscopy
high resolution electron energy loss spectroscopy
Auger electron spectroscopy
low-energy electron diffraction
electron microscopy
Molecule- and ion-mediated spectroscopies
neutron/helium diffraction
secondary ion mass spectroscopy
ion scattering spectroscopy
field-emission microscopy
Photon-mediated spectroscopies
infrared spectroscopy
Raman spectroscopy
second harmonic generation
sum frequency generation
near-edge X-ray absorption fine structure
extended X-ray absorption fine structure
solid-state spin resonance
electron spin resonance
Scanning probe microscopies
scanning tunneling microscopy
atomic force microscopy
Other techniques
Mössbauer spectroscopy
thermal desorption

By contrast, industrial catalytic reactions are carried out under ambient pressures ($\sim$ 1 atm), and surface coverages at high reaction temperatures (300–1000 K) are maintained by the high frequency of collisions between gas phase molecules and the surface. An extrapolation of results obtained in high-vacuum/low-temperature studies to high-pressure/high-temperature conditions is approximate at best, due to the pressure gap and the temperature difference.

A major direction in current catalysis research is to explore surface science techniques which can be operated at high pressure/high temperature regime. Two techniques have been adapted in our laboratory to investigate reaction mechanisms in situ under catalytic reaction con-

ditions: scanning tunneling microscopy (STM) has been used to study surface structures and infrared–visible sum frequency generation (SFG) has been applied to monitor surface reaction intermediates.

2.1. Scanning tunneling microscopy (STM)

STM is a powerful technique to monitor surface structures in situ under variable pressures at different temperatures. In the experiments, a scanning tunneling microscope is operated in a chemical reactor cell. The pressure in the reaction cell can be changed from ultra high vacuum to a few atmospheres. The substrate temperature can be also varied. The atomic structures of metal catalyst surfaces with known adsorbate coverages can be obtained under low pressures and low temperatures, and serve as references to the surface structures determined under ambient pressures and high temperatures during catalytic reactions.

Our STM studies reveal a surface reconstruction induced by chemisorption. In addition, the structure of coadsorbates on the surface can be rearranged. Upon activation, a STM tip made of transition metals can also catalyze surface reactions on a nanometer scale.

2.1.1. Chemisorption-induced surface reconstruction

Substrate atoms can be reorganized upon chemisorption in order to minimize the surface energy [18]. Fig. 3 displays STM images of a

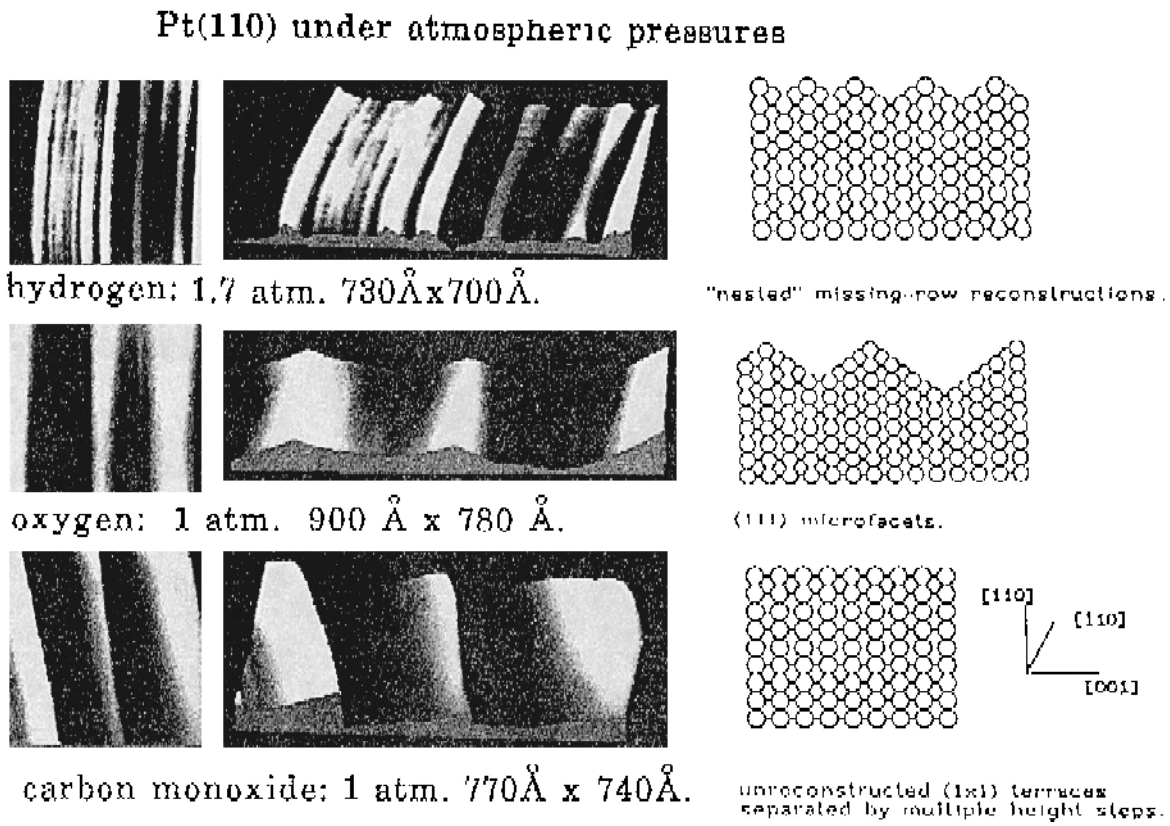

Fig. 3. Adsorbate-induced surface reconstruction of a Pt(110) surface studied in situ by STM under atmospheric pressures. Top panel: Topographic image of the Pt(110) surface in 1.6 atm of hydrogen after heating in 425 K for 5 h. Image size: 730 Å × 700 Å, vertical range $\Delta z = 10$ Å. Middle panel: Topographic image of the Pt(110) surface in 1 atm of oxygen after heating to 425 K for 5 h. Image size: 900 Å × 780 Å, $\Delta z = 25$ Å. Bottom panel: Topographic image of the Pt(110) surface in 1 atm of carbon monoxide after heating to 425 K for 4 h. Image size: 770 Å × 740 Å, $\Delta z = 42$ Å.

Pt(110) surface exposed to ambient pressures of hydrogen, oxygen and carbon monoxide at 425 K. Under 1.6 atm of hydrogen pressure, the surface presents various sizes of missing-row reconstruction. In 1 atm of oxygen, however, enlarged (111) microfacets can be observed. The surface in 1 atom of carbon monoxide appears to have large scale terraces separated by multiple height steps.

The surface reconstruction is a reversible process. The platinum surface was exposed to different gases alternatively and the surface structure changed accordingly [18]. In 1.6 atm H_2, chemisorbed oxygen reacts to form water and desorbs from the surface. In CO environment, the binding energy of hydrogen atoms on the surface is reduced and surface hydrogens are replaced by CO molecules. Under atmospheric oxygen pressure, surface CO molecules are oxidized to CO_2 and the surface is switched to be covered by oxygen. The conversion of surface structures is indicative of the adsorbate composition change on the surface.

2.1.2. Coadsorption-induced reconstruction of adsorbate overlayer

Adsorbate overlayer as well as substrate atoms can be rearranged by adsorption of coadsorbates. Surface species are highly mobile on the surface. In many cases, adsorbate structures are reorganized in order to accommodate other surface species. A reconstruction of adsorbate overlayers by coadsorption has been demonstrated in a STM and LEED study of sulfur chemisorption on Re(0001) and Pt (111) surfaces [19]. Surface structures imaged by STM are consistent with electron diffraction patterns obtained in complementary LEED studies. At a sulfur coverage of 0.25 monolayer (one atom per four substrate metal atoms), a (2×2) ordered sulfur structure can be observed, as shown in Fig. 4(a). On either Re(0001) and Pt(111) surfaces, coadsorption of carbon monoxide molecules induces a reordering of sulfur structure. The sulfur overlayer is compressed, creating empty space on the surface for carbon monoxide adsorption. The new sulfur overlayer presents a $(3\sqrt{3} \times 3\sqrt{3})R30°$ structure on Re(0001) (Fig. 4(b)) and a $(\sqrt{3} \times \sqrt{3})R30°$ structure on Pt(111). The CO molecules have a high mobility on the surface and are not visible in STM experiments. The change of sulfur overlayer structure is reversible and the original (2×2) sulfur structure can be restored after desorbing CO molecules at high temperature.

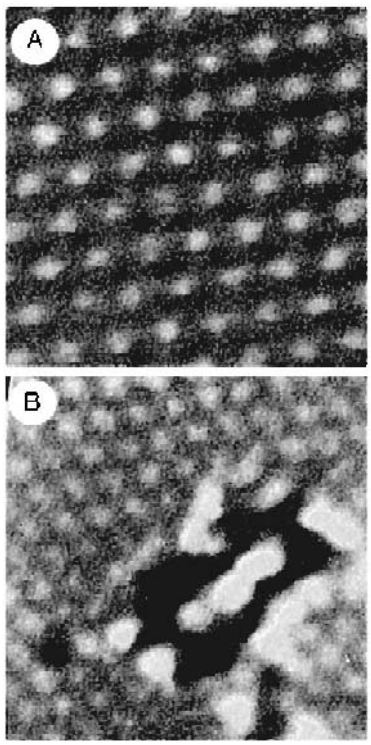

Fig. 4. STM images (a) before and (b) after the reordering of sulfur overlayer on Re(0001) induced by CO exposure. (a) The round maxima are due to individual p(2×2) ordered sulfur atoms adsorbed at the hcp hollow site of the surface. Image size: 40×40 Å. (b) A hole has formed in the p(2×2) layer where CO has adsorbed (CO molecules are not visible in the STM images, presumably due to their facile diffusion on the surface). The sulfur atoms which resided previously in the hole have been compressed to form trimers of three atoms which appear as bright spots surrounding the hole. Image size: 55×55 Å.

Competitive adsorption and mobility of adsorbates on the surface attribute to the coadsorption-induced reconstruction of adsorbate overlayers. If surface species are immobile because of a high activation energy for surface diffusion, coadsorption cannot take place. On the other

hand, the adsorption energy of one adsorbate must be sufficient to compress the other adsorbate into a more compact layer. If coadsorbates have a very low heat of adsorption, the thermodynamic driving force for adsorbate overlayer reconstruction is absent.

2.1.3. Nanocatalysis by a platinum–rhodium STM tip

A catalytic reaction on the nanometer scale is observed by scanning an activated platinum–rhodium STM tip over a Pt(111) surface inside a reactor of propylene/H_2 mixture. Propylene adsorbs via a partial dehydrogenation on Pt(111) at room temperature. The surface species is highly mobile and not visible in STM scans (Fig. 5(A)). At high temperatures ($>$ 550 K), a carbonaceous C_xH_y overlayer is produced on the surface by decomposition of propylene. As shown in Fig. 5(B), clusters have regular diameters and covers the entire span of platinum terraces ($\sim$ 100 Å). A tip-induced catalysis is initiated when the platinum–rhodium tip is activated by pulses of several tenths of a volt. As the catalytically active tip scans over the surface, the carbonaceous clusters are removed and only steps of the platinum surface are visible in STM images (Fig. 6(A)). The activated tip has a lifetime of minutes before it is deactivated (Fig. 6(B)), presumably by contamination [20].

We believe that the catalytic action by the Pt–Rh tip consists of a H_2 dissociation on the STM tip and a hydrogenation of the carbon clusters on the surface (Fig. 7). Once hydrogenated, the clusters are dissolved and remain invisible to the STM. This could be a result of either desorption of the hydrogenated fragments or their rapid diffusion on the surface at room temperature.

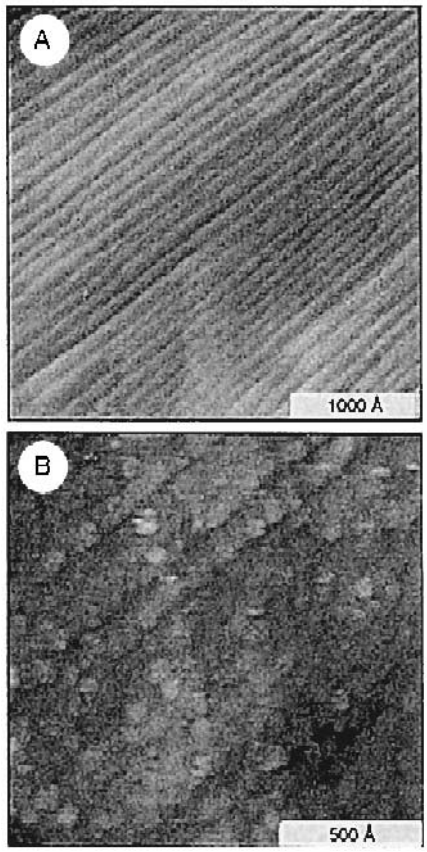

Fig. 5. STM images of a Pt(111) surface covered with hydrocarbon species generated by exposure to propylene gas. Images taken in constant- height mode at 0.1 V bias and 1.3 nA of current. (A) After adsorption at room temperature, the propylidyne species that formed was too mobile on the surface to be visible. The surface looks similar to that of the clean surface. Terrace ($\sim$100 Å wide) and monatomic steps are the only visible features. (B) After heating the adsorbed propylidyne to 500 K, clusters are formed by polymerization of the C_xH_y fragments. The clusters are of approximately round shape with a diameter equal to the terrace width.

2.2. Sum frequency generation (SFG)

Infrared–visible sum frequency generation (SFG) is an interface *specific* vibrational spectroscopy technique [21]. It is ideal for studies of surface reaction intermediates at variable temperature and variable reactant pressures. Although a few other surface vibrational spectroscopies provide satisfactory results for surface chemistry studies under vacuum, their applications under high gas pressures are seriously limited. For example, high resolution electron energy loss spectroscopy (HREELS) uses an electron beam as probe and can be only operated under a high vacuum. Transmission and reflection infrared spectroscopies pick up gas phase intensities along the optical path under

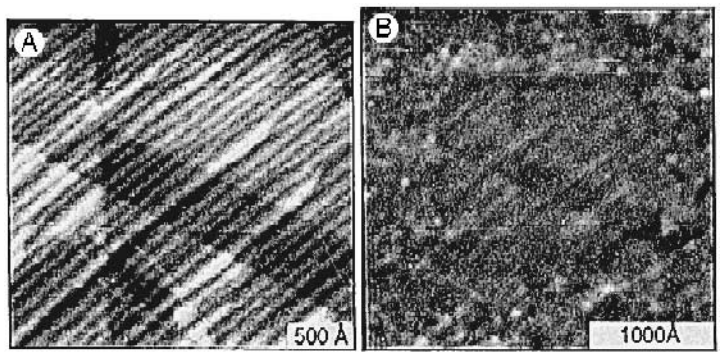

Fig. 6. The catalytic action of the STM Pt–Rh tip on a Pt(111) surface covered by carbonaceous clusters. The clusters are formed by polymerization of C_xH_y fragments after heating the adsorbed propylidyne to 550 K. Images were collected in 1 atm of propylene/H_2 (10:90) mixture. The Pt–Rh tip was activated by applying a voltage pulse of 0.9 V. (A) Surface scanned by a catalytically active tip. All the clusters were removed. (B) A slightly larger image of the area shown in (A) (center square of this image), obtained after the tip was 'deactivated', presumably by contamination. The active tip has a lifetime on the order of minutes.

high pressures. By contrast, sum frequency generation (SFG) generates virtually no signal from the gas phase and bulk material. It is arguably the most suitable technique for monitoring submonolayer concentrations of surface intermediates in situ during heterogeneous catalytic reactions on single crystals.

In an infrared–visible SFG study of catalytic reactions, a batch reactor is filled by atmospheric pressures and reaction rate is monitored by a gas chromatograph. The surface is illuminated with two high-intensity lasers: a green light and a tunable infrared beam. Photons of sum frequency are generated at the gas–solid interface (Fig. 8). By monitoring the sum frequency signal as a function of incident infrared photon energy, a vibrational spectrum of surface species can be obtained [22]. Below we describe applications of SFG on alkene hydrogenation reaction studies.

2.2.1. Ethylene hydrogenation on Pt(111)

Ethylene hydrogenation reaction on platinum surfaces is one of the simplest catalytic reactions. The reaction takes place at room temperature. As shown in Fig. 9, a reaction mechanism proposed by Horiuti and Polanyi suggests that ethylene is hydrogenated stepwise by H atoms on the surface. In absence of hydrogen, several distinct species have been identified in UHV conditions for an ethylene monolayer absorbed on Pt(111). At temperatures below 50 K, monolayer molecules interact weakly with the surface via a π-coordination. Ethylene is physisorbed

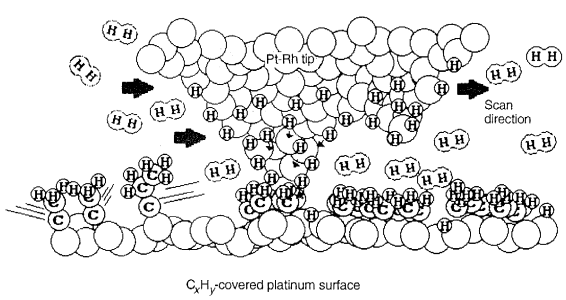

Fig. 7. The proposed model for the catalytic action by the active tip, which assumes a Pt–Rh tip with atomized hydrogen at the apex, which hydrogenated the carbon bonds of the clusters on the surface.

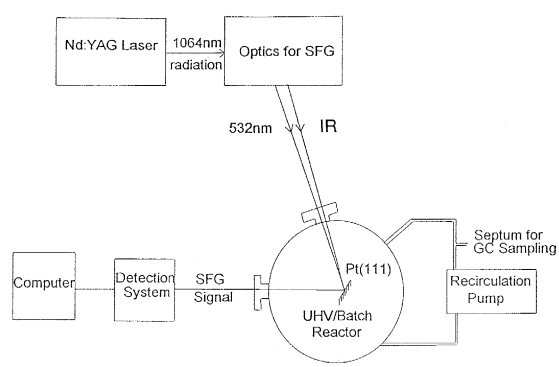

Fig. 8. The UHV/batch reactor for in situ SFG measurements.

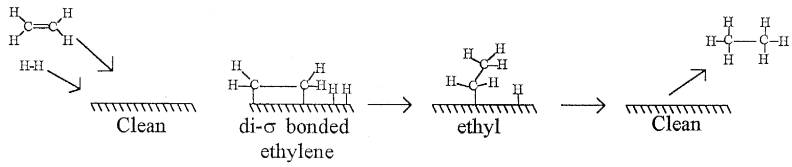

Fig. 9. Horiuti–Polanyi mechanism for ethylene hydrogenation on platinum.

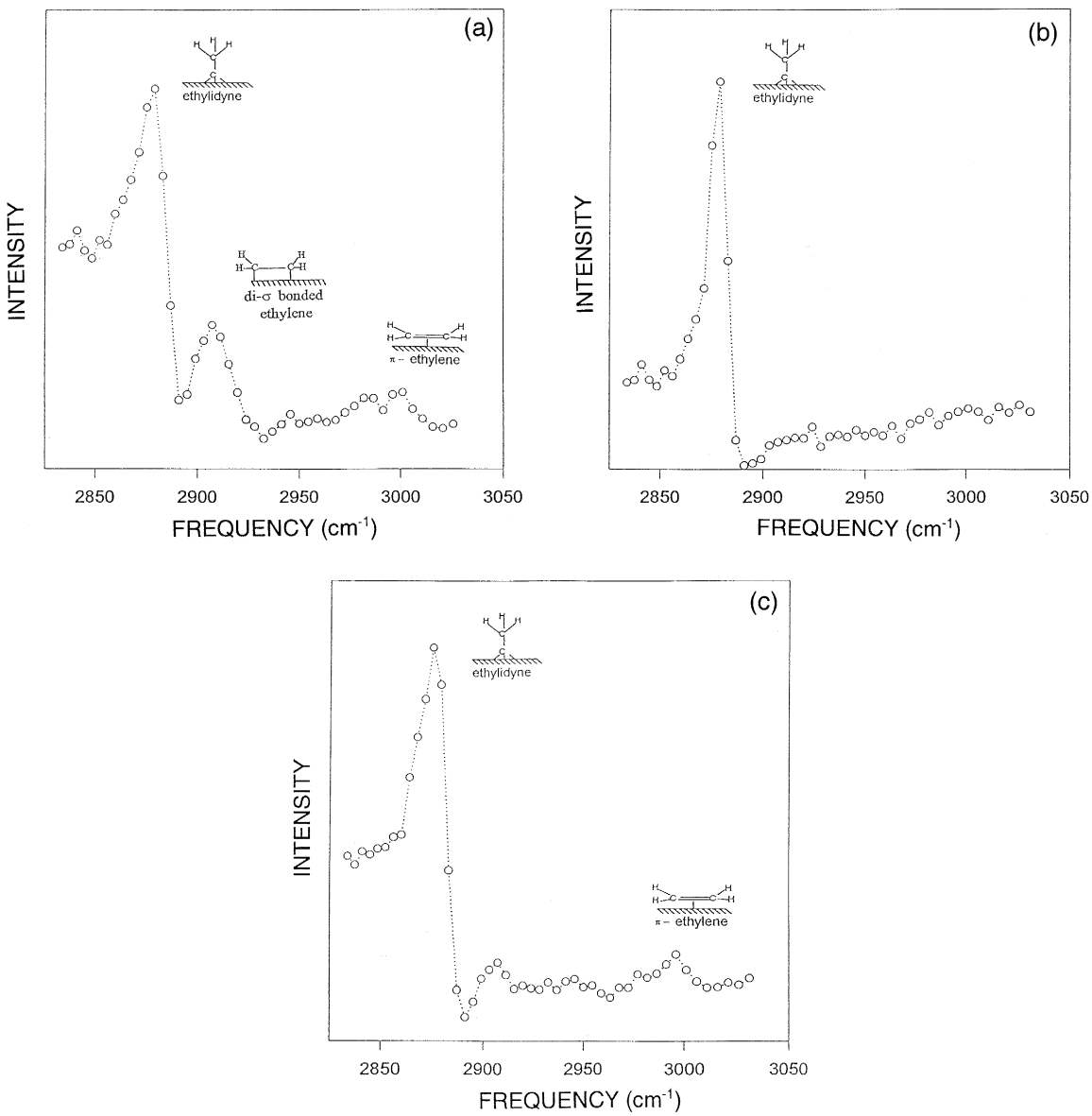

Fig. 10. (a) SFG spectrum of the Pt(111) surface during ethylene hydrogen with 100 Torr H_2, 35 Torr C_2H_4 and 615 Torr He at 295 K. (b) The vibrational spectrum of the same system after the evacuation of the reaction cell. (c) The SFG spectrum after the reactor is refilled with the same gas mixture as (a).

with its C–C bond parallel to the surface, and interatomic distance between two carbon atoms is almost unchanged with respect to the gas-phase molecule. At a temperature between 60 K and 240 K, the carbon atoms attain nearly sp^3 hybridization and bond directly to the substrate. This is referred to as di-σ bonded coordination. A further annealing of the surface induces dehydrogenation of ethylene molecules. Ethylidyne is formed by losing one hydrogen and transferring a second hydrogen atom to the other carbon, and is the prominent hydrocarbon species on surface up to 450 K.

Several groups have studied by infrared spectroscopy the reaction intermediates in the hydrogenation reaction [23–25]. All the works, however, were carried out in absence of ethylene in the gas phase. By contrast, SFG allows us to monitor surface in situ under catalytic conditions [26]. Three features present on the surface under 110 Torr H_2 and 35 Torr C_2H_4 at 295 K (Fig. 10(a)). Compared with fingerprint spectra of surface species prepared in vacuum, the peaks at 2880 cm^{-1}, 2910 cm^{-1} and the small peak around 3000^{-1} can be assigned to ethylidyne, di-σ bonded ethylene and π bonded ethylene, respectively. The weak $\nu_s(CH_2)$ signal for π-bonded molecules can be attributed to a surface-dipole selection rule for metal surface, that dynamics dipoles parallel to the surface plane are canceled by image dipoles inside the metal. The spectrum was stable for hours while the reaction rate remained constant. After the gas mixture was evacuated from the reactor, surface was saturated with ethylidyne while di-σ and π-bonded ethylene molecules disappeared (Fig. 10(b)). After the reaction cell was recharged with ethylene/H_2 mixture, the reaction rate was recovered. As shown in Fig. 10(c), π-bond ethylene was restored on the surface while the intensity from the di-σ bond species did not return. This demonstrated a direct competition for adsorption sites between the ethylidyne and di-σ bond ethylene. Since a high turnover rate was again observed in the second run in absence of di-σ-bonded species, the hydrogenation through the di-σ-bonded ethylene is at most a minor channel in the reaction scheme.

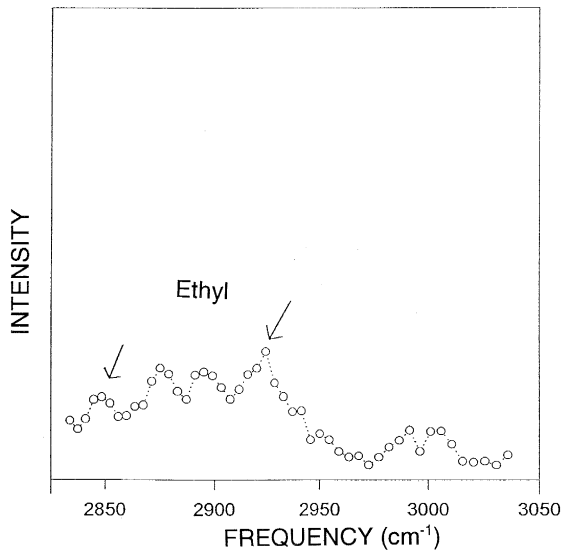

Fig. 11. SFG spectrum of ethylene hydrogenation on Pt(111) with 727 Torr H_2 and 6.0 Torr C_2H_4 at 295 K. The two peaks marked with arrows are features characteristic of an ethyl species.

It was also observed that the ethylene hydrogenation reaction occurred at the same rate regardless of the presence of ethylidyne on the surface. In addition, preadsorbed ethylidyne groups do not affect the reaction rate. It indicates that ethylidyne is not directly involved in the hydrogenation reaction. A same conclusion was reached in a transmission infrared spectroscopy study of ^{14}C ethylidyne hydrogenation in hydrogen [27].

In contrast to the behavior of di-σ-bonded ethylene and ethylidyne, the appearance of π-bonded species is directly correlated with the reaction rate. It is mostly likely to be the key intermediate in ethylene hydrogenation.

Surface ethyl groups are visible at a very high hydrogen pressures. Under 727 Torr H_2 and 6.0 Torr C_2H_4 at 295 K, two additional peaks are present on the SFG spectrum (Fig. 11). They can be assigned to an ethyl species on the surface. The low surface concentration of ethyl groups at medium hydrogen pressure regime suggests a high degree of reversibility in

the addition of the first hydrogen into adsorbed ethylene.

2.2.2. Propylene and isobutene hydrogenation on Pt(111)

Propylene [28] and isobutene [29] hydrogenation have been also studied by SFG on Pt(111) at room temperature. Similar to ethylene hydrogenation, propylene and isobutene are hydrogenated on platinum stepwise by atomic hydrogens, which are formed in hydrogen dissociation on surface. The reactions proceed via alkyl intermediates. An issue of interest is the regioselectivity of hydrogen addition to propylene and isobutene, i.e., the position selectivity of hydrogen atom addition to two nonequivalent carbon atoms in the C=C double bond. A hydrogen addition to the terminal carbon and internal carbon of propylene yields 2-propyl and 1-propyl groups, respectively (Fig. 12). Similarly, 2-isobutyl (tertiary-butyl) and 1-isobutyl groups are formed in a hydrogen addition to terminal and internal carbons of isobutene (Fig. 13).

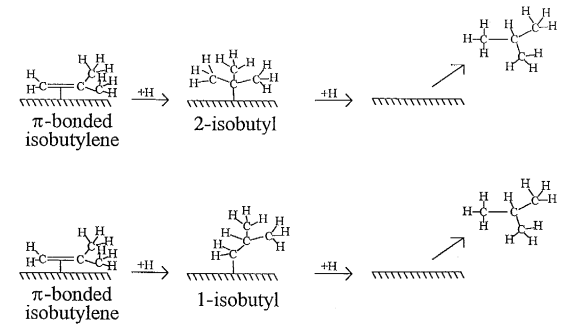

Fig. 13. Possible reaction pathways for isobutene hydrogenation on the Pt(111) surface.

Under reaction conditions of propylene hydrogenation, 2-propyl and π-bonded propylene species were observed on the surface. Vacuum studies indicated that 2-propyl and 1-propyl groups had similar hydrogenation rates. It demonstrates that the 2-propyl group is the reaction intermediate and not just a spectator residing on the surface. 2-propyl groups are formed in a preferential addition of hydrogen atom to terminal carbon in propylene molecules.

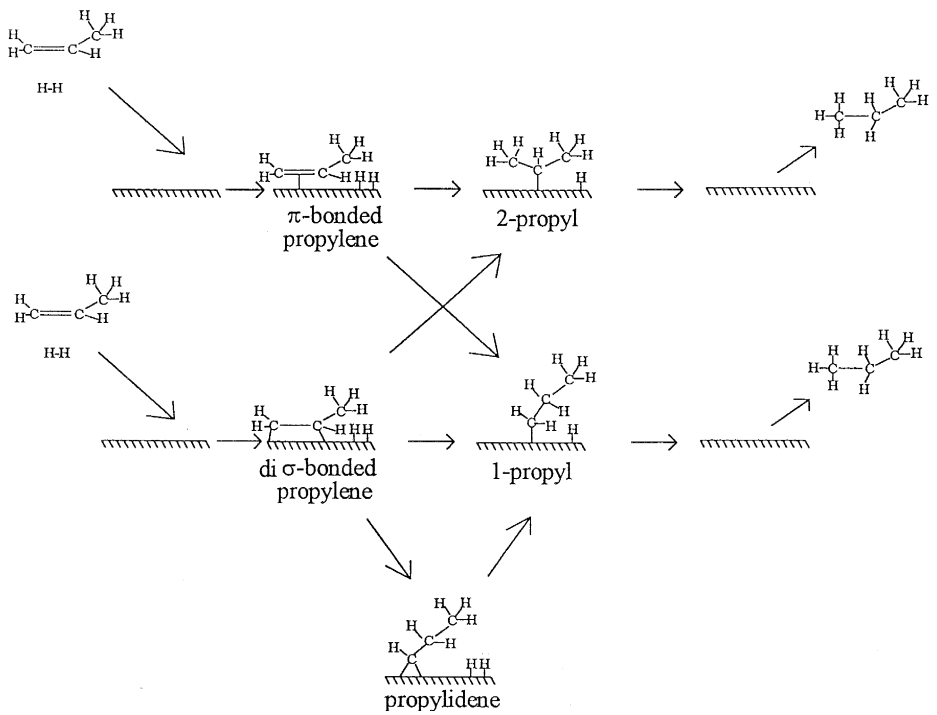

Fig. 12. Possible reaction pathways for propylene hydrogenation on the Pt(111) surface.

The isobutene hydrogenation reaction has presumably a different reaction mechanism. Although 2-isobutyl groups and π-bonded isobutene were the dominant surface species detected under reaction conditions, the hydrogenation rate of 2-isobutyl was much slower than that of 1-isobutyl. As a result, isobutene hydrogenation may be forced to proceed from π-bonded isobutene through the slow kinetic step of 1-isobutyl formation. It provides an explanation of a slow isobutene hydrogenation rate, which is at least one order of magnitude lower than for those of 1-butene and *cis*-2-butene.

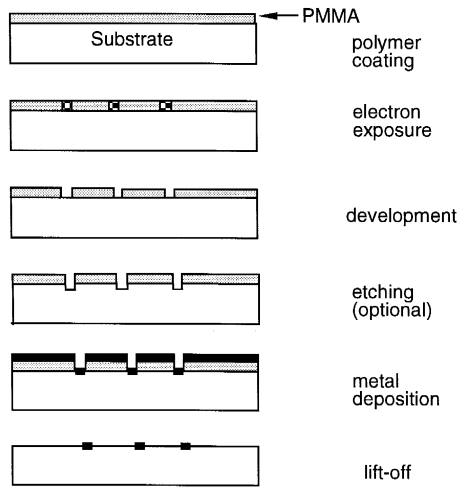

Fig. 14. A schematic diagram of the electron beam lithography process.

3. New model catalysts: fabrication of metal nanoclusters by electron beam lithography

3.1. Methodology

Although the single crystal studies are beneficial to our understanding of catalytic chemistry at the gas–solid interface, certain features of industrial supported catalysts are missing in the model system. The metal particle size has a potential influence on the catalyst reactivities. Oxide support also plays a prominent role in the catalytic reactions. A substrate-induced charge transfer to and away from the metal particles modifies their reactivity. In addition, since most catalytic reactions involve molecules diffusing between and reacting with more than one metal particle, separation between the catalyst particles can be another factor affecting catalyst performance.

One of the major challenges in modern catalysis research is to develop model *supported* catalysts. Model catalysts have to be prepared that consist of metal particles in the proper size range of 1–100 nm. A precise control of particle size and separation is desirable, which allows us to study dependence of catalyst reactivities on particle size and interparticle distance.

Fabrication of small metal particle arrays with ordered structures is now feasible using modern microelectronics technologies. Nanoscale metal catalysts with uniform size, shape and inter-particle distance can be produced by electron beam lithography. A schematic diagram of electron beam lithography process is presented in Fig. 14. A polymer (normally polymethyl methyacrylate (PMMA)) layer is first spin-coated onto the substrate. Features are ‘written’ on the polymer layer by a highly-collimated electron beam followed by dissolution of the damaged polymer. The sample is then coated by a metal thin film. After polymer remaining on the substrate is lifted off, metal particles are deposited only at positions previously registered by electron beam exposure.

Unlike many other nanofabrication technologies, lithography is a viable technique for manufacturing particles of any material on a variety of supports. Supports in industrial catalysts will be modeled by commercially available oxide surfaces: SiO_2, Al_2O_3, TiO_2, etc. The universality of the technology is essential to catalysis studies, which often requires different compositions of catalyst particle and support. By adjusting particle size, shape, spacing and support, we shall manipulate the diffusion distance of molecules, the number of active reaction sites on the surface and the electronic structure of the

catalyst. An optimization of catalyst performance can be accomplished.

UV light and X-ray radiation have also been used in lithography studies. The main advantage of electron beam lithography over the other techniques is its exceptional high resolution. It can generate features as small as a few nanometers [30]. Notice that the average particle size of industrial catalysts is 1–100 nm, electron beam lithography is, at present, the best choice in model catalyst preparation.

3.2. Reactivity tests

An initial reactivity test of metal clusters prepared by electron beam lithography has yielded encouraging results [31]. A metal cluster sample was prepared by Dr. S.J. Wind at IBM research center, Yorktown Heights. Platinum particles of 50 nm diameter and 15 nm height with 200 nm periodicity have been prepared on a 0.5×0.8 cm oxidized silicon wafer. Scanning electron microscopy (SEM) pictures of the metal cluster array are shown in Fig. 15.

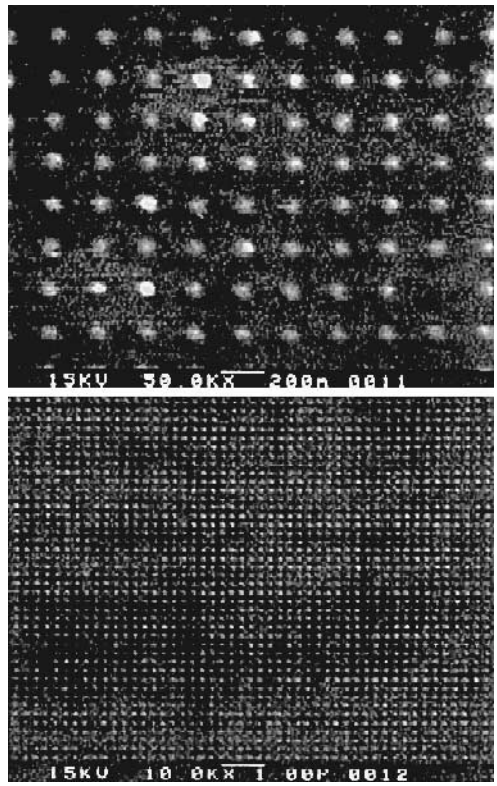

Fig. 15. SEM micrographs of platinum cluster array fabricated by electron beam lithography. The sample has a cluster size of 50 nm and a periodicity of 200 nm.

The cluster sample shows a remarkable stability upon annealing and exposure to ions and electrons. It allows us to remove surface contaminants by low energy ion sputtering and oxygen treatment. The sample can be characterized by electron- and ion-scattering surface science spectroscopies. AFM studies indicate that the sample structure remains intact after surface cleaning, catalytic reaction and sample characterization.

The rate of ethylene hydrogenation over this new model catalyst was measured in a UHV/high pressure system. The surface area of metal cluster arrays is one to two orders of magnitude smaller than a single crystal surface of comparable sample size. Fig. 16 shows the ethane yield as a function of time at room temperature, along with a background signal taken on a blank silicon wafer. The measured turnover rate is in good agreement with previous results obtained on conventional supported catalysts and single crystals. As shown in Fig. 16, an increase of reaction rate is also observed upon increasing sample temperature.

The saturation coverage of adsorbates on the platinum cluster sample can be determined from peak areas in thermal desorption studies. The thermal desorption spectra of D_2 and $^{13}C^{18}O$ from the cluster sample are displayed in Fig. 17, along with reference spectra collected on a platinum foil. The ratio of deuterium desorbing from the cluster sample to that desorbing from the reference foil sample is 2–4 times greater than the same ratio for carbon monoxide. This indicates a spillover of deuterium from platinum metal clusters onto silicon oxide support, which is a characteristic of dispersed metal catalysts.

Through the collaboration with IBM, we have accumulated valuable experience on electron beam lithography, sample handling, surface cleaning and reactivity studies of nanoscale

metal clusters. Unfortunately, the electron beam lithography machine at IBM can only fabricate features of >30 nm. They are significantly larger than industrial catalysts, which usually have an averaged size of <10 nm. A world-class electron beam lithography apparatus has been recently installed in Lawrence Berkeley National Laboratory (LBNL). The 'nanowriter' is designed with a resolution of 2.5–5 nm and a capacity to handle 8″ diameter samples. With the advances in the resolution, we shall be able to fabricate metal cluster arrays with the same structural properties as metal crystallines in industrial catalysts.

3.3. Promise

Reactivity of industrial catalysts is often modified by additives, and in many cases metal alloys are adapted as catalysts. These multicomponent catalysts can be modeled by multimetallic and alloy clusters fabricated by electron beam lithography. Particles of different constituents can be placed on the same support sequentially by repeating cycles of electron beam lithography. Electron beam lithography is also valuable to furnish high technology catalysts of variable structures. Three-dimensional metal cluster arrays of a uniform size and spacing can be also constructed. Increasing surface area is desirable in production of metal catalysts of technological significance.

Since electron beam lithography generates patterns point by point in a serial manner, at the current stage its throughput is too low to be economically practical for mass production of high technology catalysts. However, numerous low-cost, high-throughput lithographic technologies with high resolution are under development. X-ray lithography has shown a 20 nm resolution in a contact printing mode [32]. Lithographies based on scanning proximal probes have been introduced, with a resolution of about 10 nm [33]. The same resolution can be achieved by imprint lithography, which is based on a compression molding and pattern transfer process [34]. With further refinements, these lithographic technologies can support a mass production of sub-10 nm structures. It can be expected that fabrication of industrial catalysts

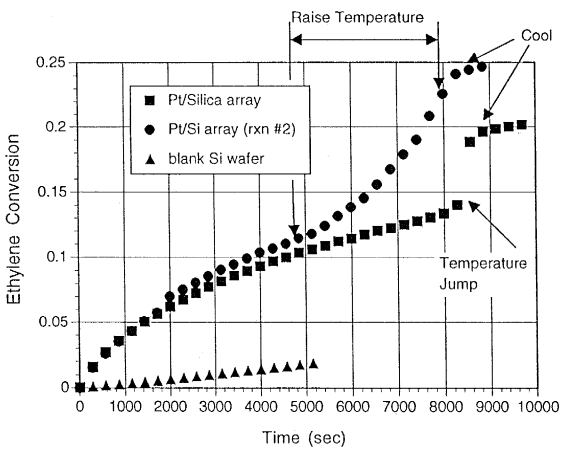

Fig. 16. Accumulated ethane yield for ethylene hydrogenation over platinum cluster array deposited on an oxidized silicon wafer. The experiment is carried out in a batch reactor coupled with a UHV system, using 1 atm hydrogen and 0.016 atm of ethylene. A background signal is collected on a silicon wafer blank. In the first reaction (squares) the sample temperature was raised rapidly from room temperature (24°C) to 75°C for 4.75 min and then cooled quickly back to room temperature. In the second reaction (circles) the sample temperature was slowly increased to 75°C over ~ 1 h before being cooled to room temperature. As shown in the figure, ethane is produced at a steady state rate of 30 s^{-1} over the platinum clusters using a geometric calculation of the surface area.

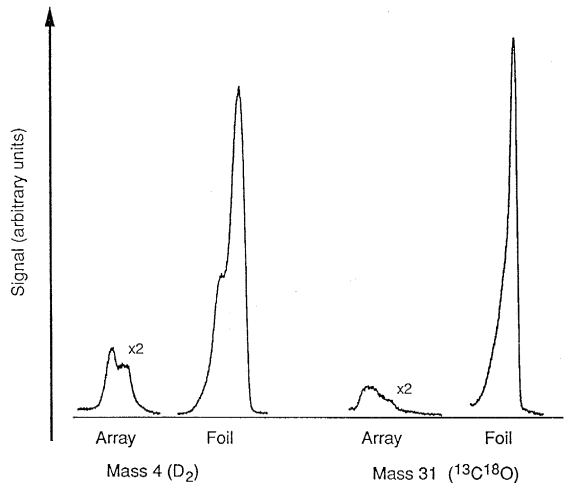

Fig. 17. Thermal desorption spectra of $^{13}C^{18}O$ and D_2 from platinum cluster array sample and a platinum foil.

with uniform structure will be a necessity in a near future and microfabrication technologies are viable for the task.

4. Other future directions

The demands of catalyst modernization and the advances of surface science technologies are governing the directions of future research, including design of new catalysts and investigation of surfaces with increasing complexity. It can be expected that an increasing spatial and time resolution in surface and adsorbate structure characterization will be among the frontiers of surface science research.

Many surface phenomena occur at a short time scale: molecule–surface collision, dissipation of translational energy, thermal accommodation of molecules on the surface, surface migration, lifetime of unreacted molecules and transient reaction intermediates on the surface at reaction temperature, etc. Time-resolved surface science technologies should be developed to address these important issues. Laser-based spectroscopies can provide the necessary time resolution (femtosecond, if necessary). Some of the techniques can be operated at high pressures (sum frequency generation, for example).

Adsorbate-induced substrate reconstruction can be both local (short range) and diffusion controlled (long range). The time scale of the process ranges from the chemisorption time scale (10^{-15} s for change transfer and 10^{-12} s for surface vibrations) to the time scale of catalytic reactions (s). It has been demonstrated that carbon monoxide oxidation to CO_2 [6,35] and ammonia reaction with NO to form N_2 and H_2O [36] show oscillatory behavior under certain temperatures and reactant pressures. The periodic surface reconstruction attributes to the oscillation of reaction rate. A time- and spatial-resolved dynamics study of substrate and adsorbate structures will be beneficial to fully understanding the surface reconstructions and their implication in heterogeneous catalysis.

The ultimate goal of catalysis research is to optimize the catalyst performance: accelerate reaction rate, increase product selectivity and inhibit catalyst deactivation. A mechanistic study of catalytic reactions will provide a basis for the design of new catalysts. The realization of the designed catalyst relies on advances in material science and chemical engineering, and involves interdisciplinary collaboration of physicists, chemists, engineers and material scientists.

It can be also anticipated that technologies and concepts developed in gas–solid interface studies will be adapted to explore other interfaces. For example, solid–liquid interfaces are involved in many important processes, including catalysis at solid–liquid interfaces, electrode reactions, reactions of colloid surfaces and a large number of biological phenomena. Laser spectroscopies, STM and solid-state NMR spectroscopy are among the techniques applicable for these studies.

Acknowledgements

This work was supported by the Director, Office of Energy Research, Office of Basic Energy Sciences, Materials Sciences Division, of the U.S. Department of Energy under Contract No. DE-AC03-76SF00098.

References

[1] H. Heinemann, A Brief History of Industrial Catalysis, in: Catalysis Science and Technology, Vol. 1 (Springer-Verlag, New York, 1981).
[2] G.A. Somorjai, Surf. Sci. 299/300 (1994) 849.
[3] D.R. Strongin and G.A. Somorjai, J. Catal. 109 (1988) 51.
[4] S.M. Davis, F. Zarea and G.A. Somorjai, J. Am. Chem. Soc. 104 (1982) 7453.
[5] A.J. Gellman, D. Neiman and G.A. Somorjai, J. Catal. 107 (1987) 92.
[6] R.C. Yeates, J.E. Turner, A.J. Gellman and G.A. Somorjai, Surf. Sci. 149 (1985) 175.
[7] J. Lahtinen and G.A. Somorjai, J. Molec. Catal. 94 (1994) 387.
[8] L.H. Dubois, P.K. Hansma and G.A. Somorjai, J. Catal. 65 (1980) 318.

[9] S.M. Davis and G.A. Somorjai, J. Catal. 65 (1980) 78.
[10] E. Segal, R.J. Madow and M. Boudart, J. Catal. 52 (1978) 45.
[11] M. Boudart, Chemtech (1986) 688.
[12] S.T. Oyama, A.M. Carr and G.A. Somorjai, J. Phys. Chem. 94 (1990) 5029.
[13] S. Fu and G.A. Somorjai, Surf. Sci. 237 (1990) 87.
[14] V. Maurice, M.B. Salmeron and G.A. Somorjai, Surf. Sci. 237 (1990) 116.
[15] G.H. Vurens, M.B. Salmeron and G.A. Somorjai, Surf. Sci. 32 (1989) 211.
[16] K.J. Williams, A.B. Boffa, M.B. Salmeron, A.T. Bell and G.A. Somorjai, Catal. Lett. 11 (1991) 77.
[17] E. Magni and G.A. Somorjai, Catal. Lett. 35 (1995) 205.
[18] B.J. McIntyre, M. Salmeron and G.A. Somorjai, J. Vac. Sci. Technol. A 11 (1993) 1964.
[19] J.C. Dunphy, B.J. McIntyre, J. Gomez, D.F. Ogletree, G.A. Somorjai and M.B. Salmeron, J. Chem. Phys. 100 (1994) 6092.
[20] B.J. McIntyre, M. Salmeron and G.A. Somorjai, Science 265 (1994) 1415.
[21] Y. Shen, Nature 337 (1989) 519.
[22] P.S. Cremer and G.A. Somorjai, Res. Sci. Instrum. submitted.
[23] T. Beebe and J. Yates Jr., J. Am Chem. Soc. 108 (1986) 663.
[24] S. Mohsin, M. Trenary and H. Robota, J. Phys. Chem. 92 (1988) 5229.
[25] J. Rekoske, R. Cortright, S. Goddard, S. Sharma and J. Dumesic, J. Phys. Chem. 96 (1992) 1880.
[26] P.S. Cremer, X. Su, Y.R. Shen and G.A. Somorjai, J. Am. Chem. Soc. in press.
[27] S. Davis, F. Zarea, B. Gordon and G.A. Somorjai, J. Catal. 92 (1985) 250.
[28] P.S. Cremer, X. Su, Y.R. Shen and G.A. Somorjai, J. Phys. Chem., submitted.
[29] P.S. Cremer, X. Su, Y.R. Shen and G.A. Somorjai, J. Chem. Soc. Faraday Trans., submitted.
[30] P.B. Fischer and S.Y. Chou, Appl. Phys. Lett. 62 (1993) 2989.
[31] P.W. Jacobs, F.H. Ribeiro, G.A. Somorjai and S.J. Wind, Phys. Rev. Lett., submitted.
[32] K. Early, M.L. Schattenburg and H.I. Smith, Microelectron. Eng. 11 (1990) 317.
[33] N. Kramer, M. Brik, J. Jorvitsma and S. Schronenberger, Appl. Phys. Lett. 66 (1995) 1325.
[34] S.Y. Chou, P.R. Krauss and P.J. Renstrom, Science 272 (1996) 85.
[35] G. Ertl, Catal. Lett. 9 (1991) 219.
[36] T. Katona and G.A. Somorjai, J. Phys. Chem. 96 (1992) 5465.